

# Unexpected diversity and novel features within a family of new azide-bridged Mn<sup>II</sup> complexes of pyridyl/imine ligands

Tapan K. Karmakar,<sup>a</sup> Guillem Aromí,<sup>\*b</sup> Barindra K. Ghosh,<sup>a</sup> A. Usman,<sup>c</sup> Hoong-Kun Fun,<sup>c</sup> Talal Mallah,<sup>d</sup> U. Behrens,<sup>e</sup> Xavier Solans<sup>f</sup> and Swapan K. Chandra<sup>\*ag</sup>

Received 27th July 2005, Accepted 17th October 2005

First published as an Advance Article on the web 4th November 2005

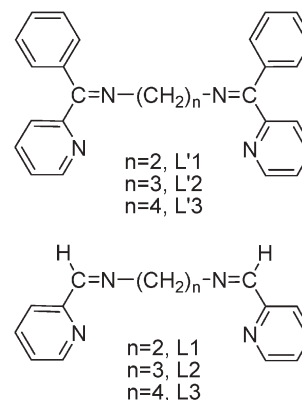
DOI: 10.1039/b510701f

A family of tetradentate ligands, [*N,N'*-bis(pyridine-2-yl)]ethane-1,2-diamine (L1), [*N,N'*-bis(pyridine-2-yl)]propane-1,3-diamine (L2) and [*N,N'*-bis(pyridine-2-yl)]butane-1,4-diamine (L3) has been prepared. These ligands differ only in the number of CH<sub>2</sub> groups separating two pyridyl/imine moieties, however, in reactions with Mn<sup>II</sup> and N<sub>3</sub><sup>-</sup> salts, they produce structurally very diverse solids; [Mn<sub>2</sub>(L1)<sub>3</sub>(N<sub>3</sub>)<sub>n</sub>](ClO<sub>4</sub>)<sub>3n</sub> (**1**), [Mn<sub>2</sub>(L2)<sub>2</sub>(N<sub>3</sub>)<sub>2</sub>](PF<sub>6</sub>)<sub>2</sub> (**2**) and [Mn<sub>2</sub>(L3)(N<sub>3</sub>)<sub>2</sub>](ClO<sub>4</sub>)<sub>2n</sub> (**3**). Complexes **1**, **2** and **3** consist of azido-bridged magnetically dilute Mn<sub>2</sub> pairs, arranged as 1-D, discrete and 2-D arrays, respectively. In these materials, the connection between Mn centers within the dinuclear entities occurs through mono-1,3-N<sub>3</sub><sup>-</sup>, bis-1,3-N<sub>3</sub><sup>-</sup> and bis-1,1-N<sub>3</sub><sup>-</sup> bridges, respectively, for **1**, **2** and **3**. Bulk magnetic measurements reveal that the coupling within such units is antiferromagnetic ( $J = -1.8 \text{ cm}^{-1}$ , **1**;  $J = -4.8 \text{ cm}^{-1}$ , **2**) and ferromagnetic ( $J = +1.45 \text{ cm}^{-1}$ , **3**), depending on whether the N<sub>3</sub><sup>-</sup> binding mode is end-to-end (EE) or end-on (EO). The reported values are given according to the convention  $H = -2JS_1S_2$  for the spin-Hamiltonian.

## Introduction

The use of azide as a bridging ligand and as a medium to propagate superexchange magnetic interactions between paramagnetic centers has been widely exploited in materials chemistry.<sup>1</sup> The reasons are the versatility of this ligand to bind more than one metal in a variety of modes and its capacity to mediate different types of magnetic coupling. The two most commonly observed bridging coordination modes are  $\mu_2$ -1,1 (end-on, EO) and  $\mu_2$ -1,3 (end-to-end, EE), which, most of the time, facilitate ferro- and antiferromagnetic exchange, respectively. A main goal in the area of molecular magnetism is the preparation of new discrete or extended coordination compounds exhibiting large spin numbers by establishing ferromagnetic interactions between spin carriers. This has been sought by, for example, combining within chemical reactions the ligand azide and the ion Mn<sup>II</sup>, which often hosts five unpaired electrons. A large number of systems with great structural diversity have been prepared in this manner, where the precise coordination mode of the N<sub>3</sub><sup>-</sup> group, the connectivity between the metals and the dimensionality of

the system depends primarily on the nature of the co-ligand used. Thus extended architectures featuring the EO<sup>2-5</sup> or the EE<sup>2,6-9</sup> coordination mode have been reported, as well as systems combining both.<sup>4,10-13</sup> Some remarkable examples are the only homometallic ferrimagnetic 1-D extended system ever prepared and characterized to date<sup>14</sup> or the observation of spontaneous resolution of a chiral 2-D crystalline network containing azide and a non-chiral ligand.<sup>15</sup> Surprisingly, however, only very few examples of discrete Mn<sup>II</sup> species containing N<sub>3</sub><sup>-</sup> have been reported. There are two reports of bis- $\mu_2$ -1,1-azido dinuclear complexes<sup>16,17</sup> and only two examples of  $\mu_2$ -1,3-azido bridged dimmers of Mn<sup>II</sup>,<sup>18,19</sup> whereas the [Mn-( $\mu_2$ -1,3-N<sub>3</sub>)<sub>2</sub>-Mn] moiety has not yet been described within a molecular species. We recently reported on the reactivity of a family of three pyridyl/imine based ligands (L'1 to L'3 in Scheme 1) with sources of both, Mn<sup>II</sup> and N<sub>3</sub><sup>-</sup>. Interestingly, in the three cases discrete ferromagnetically



Scheme 1 Imine/pyridyl ligands.

<sup>a</sup>Department of Chemistry, The University of Burdwan, Burdwan, 713104, India. E-mail: dr\_swapan@sify.com; Fax: +91 342 2557938

<sup>b</sup>Universitat de Barcelona, Departament de Química Inorgànica, Diagonal 647, Barcelona, 08028, Spain. E-mail: guillem.aromi@qi.ub.es; Fax: +34 93 4907725;

<sup>c</sup>X-Ray Crystallography Unit, School of Physics, Universiti Sains Malaysia, 11800 USM, Penang, Malaysia

<sup>d</sup>Laboratoire de Chimie Inorganique, Université Paris-Sud, Bat. 420, UMR CNRS 8613, 91405 Orsay, France

<sup>e</sup>Institute Anorgan. und Angew. Chem, Martin Luther King Pl 6, D 2016, Germany

<sup>f</sup>Departament de Cristallografia i Mineralogia, Universitat de Barcelona, Martí i Franquès s/n, 08028, Barcelona, Spain

<sup>g</sup>Department of Chemistry, Visva Bharati, Santiniketan, 731235, India

coupled dinuclear species with a  $[\text{Mn}-(\mu\text{-}1,1\text{-N}_3)_2\text{-Mn}]^{2+}$  core were obtained.<sup>17</sup> In a previous report, it had been shown that derivatives of these ligands with  $n = 0$  (see Scheme 1) and various substituents on the C-atom of the C=N group led to a variety of 1-D and 2-D  $\text{Mn}^{\text{II}}\text{-N}_3^-$  architectures with interesting magnetic and optical properties.<sup>15</sup> We have now systematically studied the reactivity of the related series L1 to L3 (Scheme 1) towards mixtures containing  $\text{Mn}^{\text{II}}$  and  $\text{N}_3^-$ . Surprisingly, the mere replacement of phenyl substituents by hydrogen atoms on the C=N functionality leads, instead of ferromagnetic dinuclear molecules, to a variety of structures with different dimensionality. These include a 1-D polymer of ( $\mu\text{-}1,3$ -azido)  $\text{Mn}_2$  moieties,  $[\text{Mn}_2(\text{L}1)_3(\text{N}_3)]_n(\text{ClO}_4)_{3n}$  (**1**), the first reported discrete bis-( $\mu\text{-}1,3$ -azido)  $\text{Mn}^{\text{II}}$  dimer,  $[\text{Mn}_2(\text{L}2)_2(\text{N}_3)_2](\text{PF}_6)_2$  (**2**), and a unique 2-D network of bis-( $\mu\text{-}1,1$ -azido)  $\text{Mn}_2$  units,  $[\text{Mn}_2(\text{L}3)(\text{N}_3)_2]_n(\text{ClO}_4)_{2n}$  (**3**). The magnetic properties of this diverse group of compounds have been investigated.

## Experimental

### Synthesis

All manipulations were performed under aerobic conditions using reagents and solvents as received. Ethylenediamine, 1,3-diaminopropane, 1,4-diaminobutane, pyridine-2-carboxaldehyde and sodium azide were purchased from Lancaster and used as received. All other solvents and chemicals were of analytical grade.

**CAUTION:** Perchlorate salts and azido compounds are potentially explosive especially in the presence of organic compounds. They must be prepared and handled in small amounts, and with special care.

### Preparation of ligands

$[N,N'$ -Bis(pyridine-2-yl)ethane-1,2-diamine (L1),  $[N,N'$ -bis(pyridine-2-yl)]propane-1,3-diamine (L2) and  $[N,N'$ -bis(pyridine-2-yl)]butane-1,4-diamine (L3) were prepared *via* condensation reactions similar to those previously reported for a similar ligand.<sup>17</sup> Ethylenediamine (0.60 g, 10 mmol, L1), 1,3-diaminopropane (0.74 g, 10 mmol, L2) or 1,4-diaminobutane (0.88 g, 10 mmol, L3) and pyridine-2-carboxaldehyde (2.14 g, 20 mmol) were refluxed in 20 mL dehydrated ethanol for 6–9 h. The respective ligands were isolated after evaporating the solvent and were recrystallized from EtOH–H<sub>2</sub>O (5 : 1 of volume ratio). The products were isolated as brown waxy materials after drying in vacuum over P<sub>4</sub>O<sub>10</sub>. The yields were 2.30 g (*ca.* 97%), 2.40 g (*ca.* 95%) and 2.85 g (*ca.* 94%) for L1, L2 and L3, respectively. Analytical data calcd for C<sub>14</sub>H<sub>14</sub>N<sub>4</sub> (L1): C, 70.57; H, 5.92; N, 23.51. Found: C, 70.46; H, 5.81; N, 23.39%. Analytical data calcd for C<sub>15</sub>H<sub>16</sub>N<sub>4</sub> (L2): C, 71.40; H, 6.39; N, 22.20. Found: C, 71.46; H, 6.31; N, 22.11%. Analytical data calcd for C<sub>16</sub>H<sub>18</sub>N<sub>4</sub> (L3): C, 72.15; H, 6.81; N, 21.04. Found: C, 72.06; H, 6.69; N, 21.09%.

**$[\text{Mn}_2(\text{L}1)_3(\text{N}_3)]_n(\text{ClO}_4)_{3n}$  (**1**).** A methanolic solution (5 mL) of ligand L1 (0.179 g, 0.75 mmol) was added dropwise to a stirred methanolic solution (12 mL) of  $\text{Mn}(\text{ClO}_4)_2 \cdot 6\text{H}_2\text{O}$

(0.181 g, 0.5 mmol) and the stirring maintained constant for 0.5 h at room temperature. To the resulting orange solution was slowly added an aqueous methanolic solution (5 mL CH<sub>3</sub>OH and 1 mL H<sub>2</sub>O) of sodium azide (0.016 g, 0.25 mmol). The resulting orange solution was left undisturbed to slowly evaporate. After 3 weeks, an orange crystalline compound was obtained by filtration, washed with methanol and dried in vacuum desiccators. The yield was *ca.* 54% (0.16 g). Analytical data calcd for C<sub>42</sub>H<sub>42</sub>N<sub>15</sub>O<sub>12</sub>Cl<sub>3</sub>Mn<sub>2</sub>: C, 43.29; H, 5.92; N, 18.03, Mn, 9.43%. Found: C, 43.34; H, 5.86; N, 18.11; Mn, 9.32%.

**$[\text{Mn}_2(\text{L}2)_2(\text{N}_3)_2](\text{PF}_6)_2$  (**2**).** To an ethanolic solution (10 mL) of  $\text{MnCl}_2 \cdot 4\text{H}_2\text{O}$  (0.050 g, 0.25 mmol) was added ligand L2 (0.063 g, 0.25 mmol) in methanol (6 mL) over a period of 15 min. To the resulting yellow–orange solution, an aqueous ethanolic solution (2 mL C<sub>2</sub>H<sub>5</sub>OH and 2 mL H<sub>2</sub>O) of sodium azide (0.016 g, 0.25 mmol) was added slowly followed by addition of an aqueous ethanolic solution (2 mL C<sub>2</sub>H<sub>5</sub>OH and 2 mL H<sub>2</sub>O) of ammonium hexafluorophosphate (0.082 g, 0.50 mmol). The solution was then filtered, an insoluble precipitate was discarded and the filtrate was left undisturbed to slowly evaporate. After 6–7 d, yellowish-green needle-shaped crystals of **2** were obtained in *ca.* 80% yield (0.10 g). Analytical data calcd for C<sub>30</sub>H<sub>32</sub>N<sub>14</sub>P<sub>2</sub>F<sub>12</sub>Mn<sub>2</sub>: C, 36.45; H, 3.26; N, 19.84, Mn, 11.11%. Found: C, 36.34; H, 3.18; N, 19.88; Mn, 11.06%.

**$[\text{Mn}_2(\text{L}3)_2(\text{N}_3)_2]_n(\text{ClO}_4)_{2n}$  (**3**).** A methanolic solution (15 mL) of ligand L3 (0.133 g, 0.50 mmol) was slowly added to a stirred warm (*ca.* 40 °C) methanolic solution (30 mL) of  $\text{Mn}(\text{ClO}_4)_2 \cdot 6\text{H}_2\text{O}$  (0.181 g, 0.50 mmol). The stirring and heating was maintained for 30 min and then an aqueous methanolic solution (5 mL CH<sub>3</sub>OH and 1 mL H<sub>2</sub>O) of sodium azide (0.033 g, 0.50 mmol) was added slowly to the mixture and the stirring maintained for another further 15 min. The resulting solution after filtration was left to stand at room temperature and it was again filtered after 2 d. After two weeks, yellow needle-shaped crystals of **3** were obtained from the filtrate in *ca.* 35% yield (0.080 g). Analytical data calcd for C<sub>16</sub>H<sub>18</sub>N<sub>7</sub>O<sub>4</sub>ClMn: C, 41.53; H, 3.92; N, 21.19, Mn, 11.87%. Found: C, 41.44; H, 3.86; N, 21.11; Mn, 11.73%.

**Physical measurements.** Elemental analyses for carbon, hydrogen and nitrogen were performed using a Perkin Elmer 2400II elemental analyzer. Manganese contents were determined by titrimetric methods. Infrared spectra (4000–400 cm<sup>-1</sup>) were recorded on KBr pellets (at 298 K) using a JASCO FT/IR-420 spectrometer. The magnetic studies were carried out on polycrystalline samples using a Quantum Design MPMS SQUID magnetometer operating in the 300–2 K temperature range and 0–5.5 Tesla. Susceptibility measurements were performed within applied fields of 3000 Oe and for compound **3** below 100 K also at 500 Oe in order to avoid saturation effects. Pascal's constants were utilized to estimate diamagnetic corrections, the value in each case being subtracted from the experimental susceptibility data to give the molar magnetic susceptibility ( $\chi_M$ ).

**Table 1** Crystallographic data for complexes **1**, **2** and **3**

Formula	<b>1</b> C <sub>42</sub> H <sub>42</sub> N <sub>15</sub> O <sub>12</sub> Cl <sub>3</sub> Mn <sub>2</sub>	<b>2</b> C <sub>30</sub> H <sub>32</sub> N <sub>14</sub> F <sub>12</sub> Mn <sub>2</sub> P <sub>2</sub>	<b>3</b> C <sub>16</sub> H <sub>18</sub> N <sub>7</sub> O <sub>4</sub> ClMn
Crystal size/mm	0.50 × 0.36 × 0.26	0.48 × 0.30 × 0.20	0.40 × 0.20 × 0.10
Fw/g mol <sup>-1</sup>	1165.12	988.52	462.76
Space group	C2/c	P2 <sub>1</sub> /c	Pbcn
a/Å	19.5706(3)	9.4938(1)	12.5606(6)
b/Å	20.7246(5)	16.1284(2)	17.2500(8)
c/Å	14.1497(3)	12.8164(1)	18.1617(9)
α (deg)	90	90	90
β (deg)	118.309(1)	94.5494(2)	90
γ (deg)	90	90	90
V/Å <sup>3</sup>	5052.65(18)	1956.26(4)	3935.1(3)
Z	4	2	8
ρ <sub>calc</sub> /g cm <sup>-3</sup>	1.540	1.678	1.562
μ (Mo Kα)/mm <sup>-1</sup>	0.71073	0.830	0.846
θ <sub>min</sub> /θ <sub>max</sub> (deg)	2.56/28.31	2.03/28.00	2.24/27.50
Ind. reflections	6147 ( <i>R</i> <sub>int</sub> = 0.1317)	4680 ( <i>R</i> <sub>int</sub> = 0.1014)	4509 ( <i>R</i> <sub>int</sub> = 0.0592)
Obs. reflections [ <i>I</i> > 2.0σ( <i>I</i> )]	2503	3319	3109
<i>R</i> <sup>a</sup>	0.0877	0.0453	0.0585
<i>R</i> w <sup>b</sup> , S	0.2214, 0.876	0.0980, 0.927	0.1502, 1.025

$$^a R = \sum (|F_o| - |F_c|) / \sum |F_o|; ^b wR = \{ \sum w(|F_o|^2 - |F_c|^2)^2 / \sum w(|F_o|^2)^2 \}^{1/2}.$$

**X-Ray crystallography.** Single-crystals suitable for X-ray crystallographic analysis† were selected following examination under a microscope. X-Ray data of **1** and **2** were collected at 293 K with a Siemens SMART CCD diffractometer. X-Ray data of **3** were collected at 200 K on a Bruker-AXS SMART APEX/CCD diffractometer. All data collections were carried out using Mo Kα radiation ( $\lambda = 0.71073$  Å) in an  $\omega - 2\theta$  scan mode. 14478 reflections were collected for **1**, of which 6147 were independent (*R*<sub>int</sub> = 0.1317); 13359 reflections for **2**, of which 4680 were independent (*R*<sub>int</sub> = 0.1014) and 44314 reflections for **3**, of which 4509 were independent (*R*<sub>int</sub> = 0.059). The intensity data were corrected for Lorentz and polarization effects. Empirical absorption corrections were made based on psi-scans<sup>20</sup> for **1** and **2** and using the SADABS program for **3**.<sup>21</sup> The structures were solved by direct methods and the structure solution and refinement was based on  $|F|^2$ . All non-hydrogen atoms were refined with anisotropic displacement parameters. Even when located in the Fourier map, hydrogen atoms were placed in calculated positions and given isotropic *U* values 1.2 times that of the atom to which they are bonded. Acetonitrile hydrogen atoms were neither located nor placed in calculated positions. The atomic scattering factors and anomalous dispersion terms were taken from the standard compilation.<sup>22</sup> All crystallographic calculations were carried out using SHELX-97<sup>23</sup> and ORTEP-3<sup>24</sup> program packages. The crystal data and data collection details are gathered in Table 1.

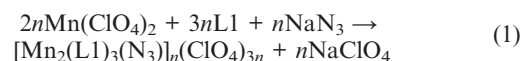
## Results and discussion

### Synthesis

Ligands L1, L2, and L3 were prepared by the analogous synthetic method to that used for the previously reported series of ligands L'1 to L'3 (Scheme 1).<sup>17</sup> As for the published system, the yields obtained for L1 to L3 were essentially

quantitative. We were interested in investigating the effect that a seemingly irrelevant modification on the ligand, namely removal of the phenyl substituent from the C atom of the C=N function, would have on the structure of the solids resulting from reaction with the Mn<sup>II</sup>/N<sub>3</sub><sup>-</sup> system. The family of ligands L' had produced in all cases discrete bis-EO-azido bridged Mn<sub>2</sub><sup>II</sup> complexes.<sup>17</sup> However, it has been shown in the past that small changes on a co-ligand, L, may lead to dramatic modifications in structure and properties of the resulting Mn<sup>II</sup>/L/N<sub>3</sub><sup>-</sup> assemblies.<sup>14,25–27</sup>

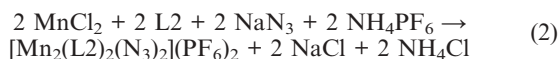
Reactions of L1 with Mn(ClO<sub>4</sub>)<sub>2</sub> and NaN<sub>3</sub> in a methanol–water mixture using various molar ratios yielded invariably an orange crystalline compound formulated [Mn<sub>2</sub>(L1)<sub>3</sub>(N<sub>3</sub>)<sub>n</sub>-(ClO<sub>4</sub>)<sub>3n</sub>] (1) on the basis of elemental analyses, infrared (IR) spectroscopy and X-ray crystallographic data. Compound **1** consists of a 1D chain of mono-EE-N<sub>3</sub><sup>-</sup> bridged Mn<sub>2</sub><sup>II</sup> pairs linked by L1 (see below), thus, the absence of the phenyl substituent induces the formation of a completely different architecture when compared with the related reaction with L'1. When the Ph group is present, the compound formed is a discrete bis-EO-N<sub>3</sub><sup>-</sup> bridged Mn<sub>2</sub><sup>II</sup> complex. There is not an apparent reason preventing the formation of such a molecular complex with L1, thus, the polymeric structure must be more stable than the discrete complex and the formation of the former with L'1 might have been prevented for steric reasons (in particular at the ligand molecule that acts as link between Mn<sub>2</sub><sup>II</sup> pairs, see below). The formation of **1** was optimized by adjusting the molar ratio of the reagents to the composition of the final product. This reaction can be described by eqn 1.



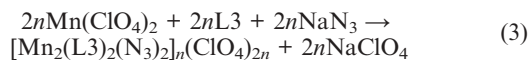
A reaction similar to that above was explored with L2, which features a propylene group in between both imine moieties. In particular, L2 was mixed with MnCl<sub>2</sub> and NaN<sub>3</sub> in the presence of NH<sub>4</sub>PF<sub>6</sub>. This led to the formation of a yellowish-green, needle-shaped crystalline product which was

† CCDC reference numbers 279584–279586. For crystallographic data in CIF or other electronic format see DOI: 10.1039/b510701f

identified by single crystal X-ray crystallography as  $[\text{Mn}_2(\text{L}2)_2(\text{N}_3)_2](\text{PF}_6)_2$  (**2**). A similar reaction with the corresponding L' ligand (L'2, Scheme 1) had also led to a dinuclear molecular species, however, with  $\text{N}_3^-$  bound as end-on. Complex **2** is in fact the first reported discrete system of  $\text{Mn}^{\text{II}}$  featuring the bis- $(\mu_2\text{-}1,3\text{-}\text{N}_3^-)$  bridge. This raises the intriguing question as to what defines the preference of EO *versus* the EE binding mode. In the present example, the steric argument is hardly applicable, since the less sterically demanding mode arises with the least encumbered ligand. Another difference in this equation that might seem unimportant is the use of a different source of  $\text{Mn}^{\text{II}}$  together with "external" addition of the counter ion  $\text{PF}_6^-$ . These factors can dramatically modify the nature of the isolated product, sometimes for solubility reasons, or because they influence in particular manners the formation of by-products that might not even be observed or identified. Eqn 2 describes the reaction leading to **2**.



When an analogous butylene ligand, L3 is allowed to react with  $\text{Mn}(\text{ClO}_4)_2$  and  $\text{NaN}_3$  in methanol–water mixtures, needle shaped crystals of a product are obtained, the identity of which was established as  $[\text{Mn}_2(\text{L}3)_2(\text{N}_3)_2]_n(\text{ClO}_4)_{2n}$  (**3**) by means of single crystal X-ray diffraction. Complex **3** comprises  $\text{Mn}_2$  units featuring two  $\mu_2\text{-}1,1\text{-}\text{N}_3^-$  bridges such as in the compound previously prepared with L'3. The recently reported complex however is a discrete molecule, with each of the multidentate ligands wrapped around one manganese center. In complex **3**, each Mn atom is linked by two L3 ligands to two other Mn centers from different  $\text{Mn}_2$  units, forming a 2-D network (see below). The optimal yield was obtained using equimolar amounts of all reagents, as summarized in eqn 3.



The reactivity just described shows that it is important to explore the diversity that might be brought by small changes on a particular ligand system. This has allowed unveiling structural moieties that had never been observed before.

### Description of structures

The identity of complexes **1**, **2** and **3** could only be established through the determination of their molecular structure by means of single-crystal X-ray diffraction. Crystallographic

**Table 2** Selected interatomic distances (Å) and angles (deg) for compound **1**; 'b' refers to symmetry operation  $[1/2 - x, 1/2 - y, -z]$

Mn(1)–N(1)	2.312(4)	Mn(1)–N(2)	2.250(6)
Mn(1)–N(3)	2.280(5)	Mn(1)–N(4)	2.258(4)
Mn(1)–N(5)	2.187(5)	N(5)–(6)	1.120(5)
N(1)–Mn(1)–N(2)	71.1(2)	N(1)–Mn(1)–N(3)	93.9(1)
N(1)–Mn(1)–N(4)	143.3(2)	N(1)–Mn(1)–N(5)	98.2(2)
N(2)–Mn(1)–N(3)	110.0(2)	N(2)–Mn(1)–N(4)	145.5(2)
N(2)–Mn(1)–N(5)	87.4(2)	N(3)–Mn(1)–N(4)	73.5(2)
N(3)–Mn(1)–N(5)	161.3(2)	N(4)–Mn(1)–N(5)	88.4(2)
Mn(1)–N(5)–N(6)	162.9(5)	N(5)–N(6)–N(5)b	180.00

**Table 3** Selected interatomic distances (Å) and angles (deg) for compound **2**; 'a' refers to symmetry operation  $[1 - x, -y, 1 - z]$

Mn(1)–N(1)	2.309(2)	Mn(1)–N(2)	2.246(2)
Mn(1)–N(3)	2.281(2)	Mn(1)–N(4)	2.289(2)
Mn(1)–N(5)	2.244(2)	Mn(1)–N(6)	2.244(2)
N(5)–N(7)a	1.169(3)	N(6)–N(7)	1.171(3)
Mn(1)⋯Mn(1)a	5.569(1)	N(1)–Mn(1)–N(2)	72.58(7)
N(1)–Mn(1)–N(3)	124.71(7)	N(1)–Mn(1)–N(4)	94.57(7)
N(1)–Mn(1)–N(5)	83.03(8)	N(1)–Mn(1)–N(6)	142.61(8)
N(2)–Mn(1)–N(3)	79.62(7)	N(2)–Mn(1)–N(4)	134.07(7)
N(2)–Mn(1)–N(5)	132.43(8)	N(2)–Mn(1)–N(6)	89.85(7)
N(3)–Mn(1)–N(4)	72.20(7)	N(3)–Mn(1)–N(5)	145.60(8)
N(3)–Mn(1)–N(6)	82.03(7)	N(4)–Mn(1)–N(5)	87.01(8)
N(4)–Mn(1)–N(6)	120.27(8)	N(5)–Mn(1)–N(6)	85.52(8)
Mn(1)–N(5)–N(7)a	127.2(2)	Mn(1)–N(6)–N(7)	139.8(2)
N(6)–N(7)–N(5)a	177.5(2)		

**Table 4** Selected interatomic distances (Å) and angles (deg) for compound **3**; 'a' refers to symmetry operation  $[1 - x, y, 3/2 - z]$

Mn(1)–N(1)	2.249(2)	Mn(1)–N(4)	2.280(3)
Mn(1)–N(6)	2.244(3)	Mn(1)–N(1)a	2.249(2)
Mn(1)–N(4)a	2.280(3)	Mn(1)–N(6)a	2.244(3)
Mn(2)–N(1)	2.218(2)	Mn(2)–N(5)	2.245(3)
Mn(2)–N(7)	2.261(3)	Mn(2)–N(1)a	2.218(2)
Mn(2)–N(5)a	2.245(3)	Mn(2)–N(7)a	2.261(3)
N(1)–N(2)	1.210(4)	N(2)–N(3)	1.144(4)
Mn(1)⋯Mn(2)	3.471(1)		
N(1)–Mn(1)–N(4)	157.3(1)	N(1)–Mn(1)–N(6)	94.86(9)
N(1)–Mn(1)–N(1)a	77.37(9)	N(1)–Mn(1)–N(4)a	84.68(9)
N(1)–Mn(1)–N(6)a	97.42(9)	N(4)–Mn(1)–N(6)	73.69(9)
N(4)–Mn(1)–N(1)a	84.68(9)	N(4)–Mn(1)–N(4)a	115.8(1)
N(4)–Mn(1)–N(6)a	97.78(9)	N(6)–Mn(1)–N(1)a	97.42(9)
N(6)–Mn(1)–N(4)a	97.78(9)	N(6)–Mn(1)–N(6)a	164.3(1)
N(1)a–Mn(1)–N(4)a	157.3(1)	N(1)a–Mn(1)–N(6)a	94.86(9)
N(4)a–Mn(1)–N(6)a	73.69(9)	N(1)–Mn(2)–N(5)	94.6(1)
N(1)–Mn(2)–N(7)	94.41(9)	N(1)–Mn(2)–N(1)a	78.68(9)
N(1)–Mn(2)–N(5)a	170.0(1)	N(1)–Mn(2)–N(7)a	98.92(9)
N(5)–Mn(2)–N(7)	73.99(9)	N(5)–Mn(2)–N(1)a	170.0(1)
N(5)–Mn(2)–N(5)a	93.0(1)	N(5)–Mn(2)–N(7)a	94.0(1)
N(7)–Mn(2)–N(1)a	98.92(9)	N(7)–Mn(2)–N(5)a	94.0(1)
N(7)–Mn(2)–N(7)a	162.8(1)	N(1)a–Mn(2)–N(5)a	94.6(1)
N(1)a–Mn(2)–N(7)a	94.41(9)	N(5)a–Mn(2)–N(7)a	73.99(9)

data for all three complexes are in Table 1, whereas selected geometric parameters are listed in Tables 2, 3 and 4.

**$[\text{Mn}_2(\text{L}1)_3(\text{N}_3)]_n(\text{ClO}_4)_{3n}$  (**1**).** Complex **1** consists of an infinite chain (Fig. 1) of equivalent  $\text{Mn}^{\text{II}}$  ions in which end-to-end  $\text{N}_3^-$  links alternate with a bridging form of the L1 ligand, which is attained after adopting a peculiar transoid

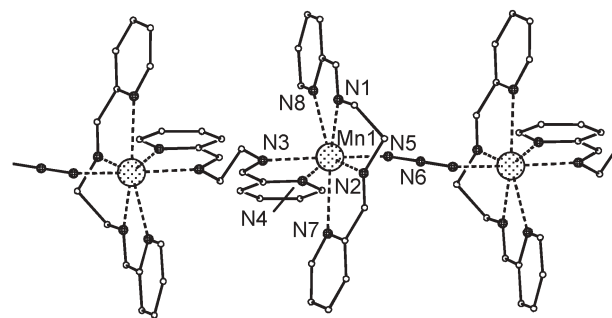


**Fig. 1** PLATON representation of  $[\text{Mn}_2(\text{L}1)_3(\text{N}_3)]_n(\text{ClO}_4)_{3n}$  (**1**), emphasizing the connectivity within the infinite chain. Hydrogen atoms have been omitted. Unique non-carbon atoms are labelled.

conformation and chelating two metals. The coordination around each metal is completed by the four N-donors of another L1 moiety, resulting in a  $[\text{MnN}_7]$  chromophore. Two of the Mn–N bonds however, are very long (2.609(6) and 2.619(4) Å) and correspond to the pyridyl N-atoms of the non-bridging L1. The remaining bond distances span the range 2.187(5) to 2.312(4). The intrachain first neighbor Mn···Mn distances are 6.547(1) and 7.650(1) Å for the  $\text{N}_3^-$  and L1 separated Mn pairs, respectively, whereas the shortest distance between metals of different chains is 8.952 Å. Since the azide ligands contain a crystallographic center of symmetry on their central atom, the N5–N6–N5b angle is exactly 180°. Each chain of **1** runs along the *c* direction of the unit cell and is linked to two other such 1-D entities located on opposite sides. This link occurs through a network of  $\pi$ – $\pi$  interactions taking place between the pyridyl rings of the non-bridging L1 ligands that interdigitate with their neighboring counterparts throughout the entire length of the chains, forming sheets of weakly bound 1-D polymers that spread on the *a*–*c* plane. These sheets are stacked on top of each other and separated by layers of  $\text{ClO}_4^-$  ions. Compounds exhibiting only one type azide bridge in form of non-interacting  $[\text{Mn}(\mu\text{-}1,3\text{-N}_3)\text{Mn}]$  moieties have been observed only once within a coordination polymer<sup>28</sup> or as discrete molecules.<sup>18,19</sup>

$[\text{Mn}_2(\text{L}2)_2(\text{N}_3)_2](\text{PF}_6)_2$  (**2**). Complex **2** (Fig. 2) is a centrosymmetric dinuclear complex of two  $\text{Mn}^{\text{II}}$  centers, each chelated by one tetradentate L2 ligand, and both mutually linked by two end-to-end  $\text{N}_3^-$  ligands. The metals are thus hexacoordinated and feature a coordination geometry closer to trigonal prismatic than to octahedral, with Mn–N distances that spread over a narrow range of 2.244(2) to 2.309(2) Å and a Mn···Mn separation of 5.569(1) Å. The positive charge is compensated by  $\text{PF}_6^-$  anions. The cycle formed by the  $[\text{Mn}_2(\text{N}_3)_2]$  core exhibits a chair conformation. The folding of this “chair” can be gauged by the angle,  $\delta$ , formed between the N–Mn–N plane and the idealized plane containing the six N atoms (Scheme 2), which in complex **2** is 16.5(1)°. The molecules of **2** interact in two directions of the space through  $\pi$ -stacking interactions of the pyridyl rings from L2, so that they are disposed in form of infinite sheets across the *b*–*c* plane, separated by  $\text{PF}_6^-$  ions. Complex **2** represents the first

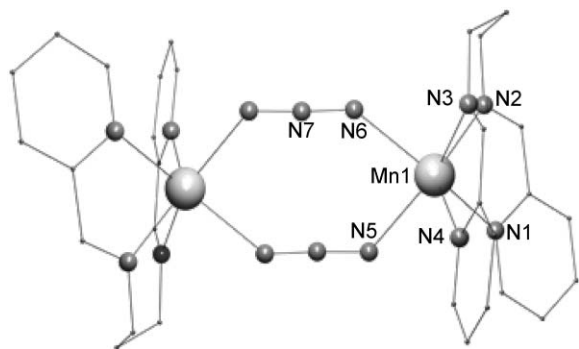
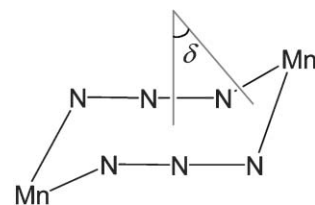


**Fig. 2** PovRay representation of  $[\text{Mn}_2(\text{L}2)_2(\text{N}_3)_2](\text{PF}_6)_2$  (**2**). Hydrogen atoms have been omitted. Unique non-carbon atoms are labelled.



**Scheme 2**

reported example of a discrete molecular system showing the double bridged unit  $[\text{Mn}(\mu\text{-}1,3\text{-N}_3)_2\text{Mn}]$ .

$[\text{Mn}_2(\text{L}3)_2(\text{N}_3)_2]_n(\text{ClO}_4)_{2n}$  (**3**). Complex **3** consists of a 2-D extended structure formed by bis- $(\mu\text{-}1,1\text{-N}_3)$  bridged  $[\text{Mn}_2^{\text{II}}]$  pairs (Fig. 3) interconnected by bridging L3 ligands (Fig. 4).

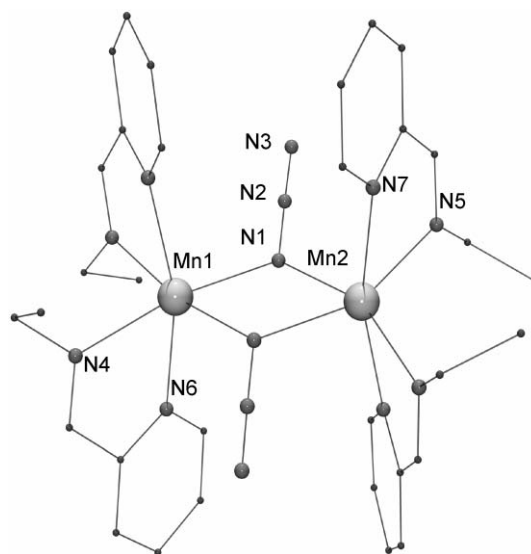


**Fig. 3** PovRay representation of  $[\text{Mn}_2(\text{L}3)(\text{N}_3)_2]_n(\text{ClO}_4)_{2n}$  (**3**) emphasizing the unique dinuclear units within the infinite sheets. Hydrogen atoms have been omitted. Unique non-carbon atoms are labelled.

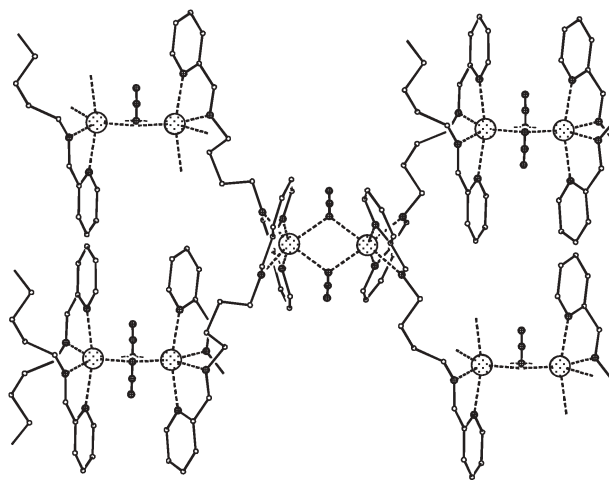


**Fig. 4** PLATON representation of  $[\text{Mn}_2(\text{L}3)(\text{N}_3)_2]_n(\text{ClO}_4)_{2n}$  (**3**) emphasizing the connectivity between dinuclear entities within the infinite chain.

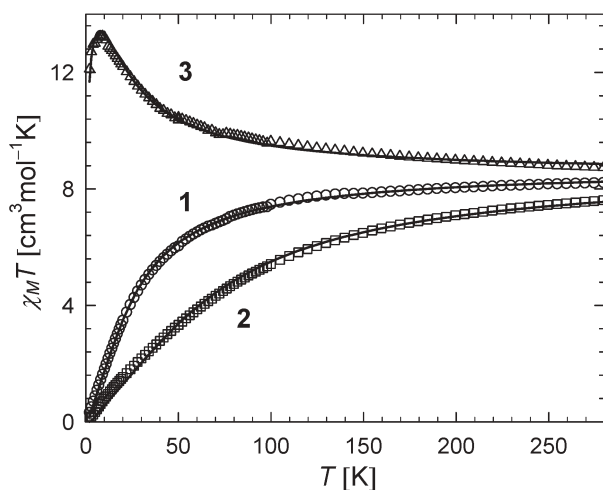


**Fig. 5** Plots of  $\chi_M T$  vs.  $T$  per mol of  $[\text{Mn}_2]$  dimeric moiety of complexes **1**, **2** and **3**. Solid lines are, respectively, the best fits to the experimental data using the appropriate model in each case (see text for details).

Each metal of these dinuclear entities is chelated by two L3 ligands *via* two of four N-donors per ligand, and bridged to two other Mn ions from adjacent dimers. Thus, each  $[\text{Mn}_2(\mu_2-1,1-\text{N}_3)_2]$  core is linked by four L3 ligands to a total of four equivalent such units. The charge in this system is compensated by two molecules of  $\text{ClO}_4^-$  per dimer of Mn. The metals in this dimer are inequivalent, exhibit a distorted octahedral environment and are located on a crystallographic  $C_2$  axis, featuring Mn–N bond distances in the range of 2.218(2) to 2.261(3) Å. The atoms of the  $[\text{Mn}_2\text{N}_2]$  core are strictly contained on a plane with Mn...Mn and N...N distances of 3.471(1) and 2.812(3) Å, and with a Mn–N–Mn angle of 102.0(1)°. The two  $\text{N}_3^-$  groups point away from opposite sides of this plane and the inclination of the azide groups with respect to the plane can be gauged by the angle N(1)–N(1a)–N(3a), which equals 37.7(1)°. The shortest intermetallic distance involving different dimers is 8.125(1) Å. The 2-D network formed by this compound spans the plane containing crystallographic axes  $a$  and  $b$  and these sheets stack along the  $c$  direction. Whereas many polymeric solids exist exhibiting the  $[\text{Mn}_2]$  fragment bridged by two end-on azide groups, it is the first time that this moiety is observed within an extended network as independent and distant pairs.

### Magnetic properties

The magnetic properties of compounds **1** to **3** were examined with a SQUID magnetometer in order to ascertain whether the structural diversity observed in this family of materials was followed by the magnetic behavior. The magnetization of all compounds was measured under a constant magnetic field of 3000 Oe in the 2–290 °C temperature range. For compound **3** additional measurements within an applied

field of 500 Oe were performed below 100 K in order to avoid the saturation effects that may appear in high-spin systems. The results are shown in Fig. 5 in form of  $\chi_M T$  vs.  $T$  plots, where  $\chi_M$  is the molar paramagnetic susceptibility per two manganese ions.

The product  $\chi_M T$  near room temperature for compound **1** is  $8.24 \text{ cm}^3 \text{ K mol}^{-1}$ , slightly below the value corresponding to two uncoupled high-spin  $\text{Mn}^{\text{II}}$  ions ( $S = 5/2$ ) with  $g = 2$  ( $8.75 \text{ cm}^3 \text{ K mol}^{-1}$ ). This value decreases slowly as the temperature is decreased, the drop becoming steeper at lower temperatures. This clearly indicates the existence of antiferromagnetic coupling between the Mn centers within the chain. The distance between adjacent  $\text{Mn}^{\text{II}}$  being too large for considering direct overlap between metallic magnetic orbitals, the coupling must be taking place *via* superexchange coupling pathways. While end-to-end  $\text{N}_3^-$  bridges are well known to mediate efficiently magnetic interactions between metallic centers, the coupling *via* an ethylenediimine bridge such as that provided by L1 in this complex is expected to be extremely weak, or nil. Thus, in order to describe quantitatively the magnetic behavior, a model was used that considered the system as an ensemble of magnetically exchanged  $\text{Mn}_2$  pairs, isolated from each other, therefore with the exchange described by the Heisenberg spin-Hamiltonian  $H = -2JS_1S_2$ , where  $S_1 = S_2 = 5/2$ ,  $J$  being the exchange coupling constant. The van Vleck equation expressing the temperature dependence of the magnetic susceptibility under such model is given in eqn 4.<sup>29</sup>

By using this equation, a very good agreement between the simulated curve (solid line on plot 1, Fig. 5) and the experimental data was obtained. The parameters obtained from the fitting procedure were  $J = -1.8 \text{ cm}^{-1}$  and  $g = 2.00$  (goodness of the fit,  $R^2 = 0.999$ ). Similar weak antiferromagnetic coupling has been observed for the only two isolated  $[\text{Mn}_2^{\text{II}}]$  complexes reported to date, exclusively bridged by the  $\mu_2-1,3-\text{N}_3^-$  moiety.<sup>18,19</sup>

Near room temperature, compound **2** exhibits a value for  $\chi_M T$  of  $7.68 \text{ cm}^3 \text{ K mol}^{-1}$ , slightly lower than **1**. The curve drops with lowering temperatures in a more pronounced manner than for the previous complex, which shows that the antiferromagnetic coupling between  $\text{Mn}^{\text{II}}$  ions in **2** is stronger than in **1**. Since this complex consists of discrete dinuclear molecules, the magnetic coupling within the molecule can be described by the spin-Hamiltonian  $H = -2JS_1S_2$ , and eqn 4 is thus appropriate for fitting the experimental data and quantitatively assessing the extent of this coupling. A fit was thus performed (solid line on plot 2 of Fig. 5) yielding best fit parameters of  $J = -4.8 \text{ cm}^{-1}$  and  $g = 2.01$  ( $R^2 = 0.997$ ). This interaction remaining rather weak, it is interesting to note that it is significantly more efficient than that observed in **1**. A plausible reason for this is that complex **2** features two exchange pathways (one per bridging ligand) as compared to only one in **1**. Since complex **2** is the first reported of its kind, it is not possible to compare

$$\chi_M = \frac{Ng^2\beta^2}{3kT} \times \frac{330 + 180e^{-10J/kT} + 84e^{-18J/kT} + 30e^{-24J/kT} + 6e^{-28J/kT}}{11 + 9e^{-10J/kT} + 7e^{-18J/kT} + 5e^{-24J/kT} + 3e^{-28J/kT} + e^{-30J/kT}} \quad (4)$$

the magnitude of the coupling with any previously reported value. However, the  $[\text{Mn}^{\text{II}}(\mu_2\text{-}1,3\text{-N}_3)_2\text{Mn}^{\text{II}}]$  moiety has been often found within 1-D polymeric structures and in several cases the magnetic within this unit has been described quantitatively. The calculated  $J$  values have been correlated to the dihedral angle,  $\theta$ , formed between the planes N–Mn–N (N-atoms bound to Mn) and the idealized plane of the six azido atoms (see Scheme 2).<sup>30</sup> The reported  $J$  values fall within the range of 3.0 to 7.7  $\text{cm}^{-1}$  (in the  $H = -2JS_1S_2$  convention) for  $\delta$  angles between 6.9 and 38.0°, and the coupling decreases as the angle gets larger. The angle in complex **2** is 16.5(1)° and  $J$  falls approximately in the region expected from this magneto-structural study. Thus, despite being a discrete system, complex **2** follows similar trends in terms of magnetic coupling as 1D extended systems with the same exchange pathways between spin carriers.

For complex **3** the product  $\chi_M T$  at room temperature is 8.73  $\text{cm}^3 \text{mol K}^{-1}$ , slightly higher than the value expected for two complexes, although still near the value expected for two independent  $\text{Mn}^{\text{II}}$  ions with  $S = 5/2$ . Contrary to both systems above, the value of  $\chi_M T$  increases as the temperature is lowered, to reach a maximum of 13.25  $\text{cm}^3 \text{mol K}^{-1}$  at 9 K. Upon further cooling, a sudden drop is observed, down to 12.12  $\text{cm}^3 \text{mol K}^{-1}$  at 2 K. These results show that within this complex the magnetic exchange is ferromagnetic. The drop at lower temperatures can be due to zero field splitting (ZFS), intermolecular antiferromagnetic interactions, or both. These two factors have the same effect on the magnetic susceptibility and very often are of the same order of magnitude, thus it is not possible to model reliably both at the same time. Approximate models contemplating the influence of either one or the other effect were considered. First, the van Vleck equation was constructed (eqn 5), as arising from the spin-Hamiltonian  $H = g\beta B(S_1 + S_2) - 2JS_1S_2$  ( $S_2 = S_1 = 5/2$ ) where the energies of the ground state ( $S_T = 5$ ) had been modified according to an axial ZFS term of the form  $H_{\text{ZFS}} = D[S_{Tz}^2 - S_T(S_T + 1)/3]$ .<sup>29</sup>

In eqn 5,  $x = D/kT$  and  $y = J/kT$ . A fit of the data using this model provided the parameters  $J = +1.45 \text{ cm}^{-1}$ ,  $g = 1.97$  and  $D = 0.04 \text{ cm}^{-1}$  ( $R^2 = 0.992$ ).

$$\chi_M = \frac{Ng^2\beta^2}{3kT} \times \frac{6e^{9x} + 24e^{6x} + 54e^x + 96e^{-6x} + 150e^{-15x} + 180e^{-10y} + 84e^{-18y} + 30e^{-24y} + 6e^{-28y}}{e^{10x} + 2e^{9x} + 2e^{6x} + 2e^x + 2e^{-6x} + 2e^{-15x} + 9e^{-10y} + 7e^{-18y} + 5e^{-24y} + 3e^{-28y} + e^{-30y}} \quad (5)$$

In the second model, a term for the interaction between molecules of the form  $zJ' <S_{Tz}> S_{Tz}$  was included in the spin-Hamiltonian, according to the molecular field approximation ( $J'$  being the interaction between molecules,  $z$  the number of first neighbours and  $<S_{Tz}>$  the mean value of the operator  $S_{Tz}$ ).<sup>29</sup> The expression that results for the temperature dependence of the paramagnetic susceptibility is below (eqn 6 and 7).

$$\chi_M = \frac{Ng^2\beta^2}{3k} \times \left[ \frac{F(J,T)}{T - (zJ'F(J,T)/3k)} \right] \quad (6)$$

$$F(J,T) = \frac{330e^{30y} + 180e^{20y} + 84e^{12y} + 30e^{6y} + 6e^{2y}}{11e^{30y} + 9e^{20y} + 7e^{12y} + 5e^{6y} + 3e^{2y} + 1} \quad (7)$$

In these equations,  $y = J/kT$  and the rest of the terms have their usual meaning. The parameters obtained from a fit using this model are  $J = +1.46 \text{ cm}^{-1}$ ,  $g = 1.97$  and  $zJ' = -0.03 \text{ cm}^{-1}$  ( $R^2 = 0.993$ ). Even if the models used are approximate, both of the above fits are rather satisfactory and provided essentially identical values of their common parameters, however, the latter was slightly better and was therefore the one used in the representation for Fig. 5. These results corroborate the established fact that the  $\text{N}_3^-$  ligand mediates (almost exclusively) ferromagnetic coupling between metals when bound in the end-on mode. We recently reported a series of discrete dinuclear complexes with core very similar to the magnetic pairs present in **3**. All were ferromagnetically coupled and a correlation between  $J$  and the Mn–N–Mn angle was observed. The coupling in **3** (with Mn–N–Mn of 101.98°) shows a similar trend as in that family, but it is significantly off the reported correlation. Additional data points are necessary in order to understand the subtleties of this possible relationship.

## Conclusions

The solid-state structural diversity of the series of  $\text{Mn}^{\text{II}}$  azide-bridged compounds synthesized and characterized with the pyridyl/imine ligands L1, L2 and L3 is in contrast with the monotony seen for the group of complexes previously formed with the analogous set of ligands L'1, L'2 and L'3. This underscores the importance of exploring the effect that small changes on the co-ligand, L, have on the structure and properties of the resulting assembly from  $\text{Mn}^{\text{II}}/\text{N}_3^-/\text{L}$  reaction systems. Thus, three very different compounds have been prepared by using three ligands differing only in the number of  $\text{CH}_2$  groups separating two pyridyl/imine moieties. These compounds consist of discrete ( $[\text{Mn}_2(\text{L}2)_2(\text{N}_3)_2](\text{PF}_6)_2$ , **2**), 1-D ( $[\text{Mn}_2(\text{L}1)_3(\text{N}_3)]_n(\text{ClO}_4)_{3n}$ , **1**) and 2-D ( $[\text{Mn}_2(\text{L}3)_2(\text{N}_3)_2]_n(\text{ClO}_4)_{2n}$ , **3**) assemblies, respectively, all unprecedented and featuring magnetically isolated  $\text{Mn}_2$  azide bridged pairs. Of particular interest are compounds **2** and **3**, the first synthesized discrete Mn complex incorporating the bis- $(\mu_2\text{-}1,3\text{-N}_3^-)$  bridging moiety and the first system featuring magnetically dilute  $[\text{Mn}_2(\mu\text{-EE-N}_3)_2]$  units as a part of an extended coordination network. Magnetic studies corroborate the ferromagnetic nature of the coupling mediated by EO  $\text{N}_3^-$  bridges (complex **3**) and the antiferromagnetic coupling existing between EE  $\text{N}_3^-$  bridged metal pairs (complexes **1** and **2**).

## Acknowledgements

This work was supported by grants from the Department of Science and Technology (Grant No. SR/S1/IC-22/2003), Government of India and the Council of Scientific and Industrial Research (Grant No. 01(1836)/03/EMR-II), New Delhi. T. K. K. thanks University Grants Commission, New Delhi, for a teacher fellowship. H. K. F thanks the Malaysian Government and Universiti Sains Malaysia for research grant R&D No. 305/PFIZIK/610961. GA thanks the Spanish Ministry of Science and Technology for a “Ramón y Cajal” research contract.

## References

- 1 J. Ribas, A. Escuer, M. Monfort, R. Vicente, R. Cortes, L. Lezama and T. Rojo, *Coord. Chem. Rev.*, 1999, **195**, 1027.
- 2 M. A. M. Abu-Youssef, A. Escuer, D. Gatteschi, M. A. S. Goher, F. A. Mautner and R. Vicente, *Inorg. Chem.*, 1999, **38**, 5716.
- 3 M. A. S. Goher, J. Cano, Y. Journaux, M. A. M. Abu-Youssef, F. A. Mautner, A. Escuer and R. Vicente, *Chem. Eur. J.*, 2000, **6**, 778.
- 4 G. DeMunno, M. Julve, G. Viau, F. Lloret, J. Faus and D. Viterbo, *Angew. Chem., Int. Ed. Engl.*, 1996, **35**, 1807.
- 5 R. Cortes, M. K. Urriaga, L. Lezama, J. L. Pizarro, M. I. Arriortua and T. Rojo, *Inorg. Chem.*, 1997, **36**, 5016.
- 6 F. A. Mautner, R. Cortes, L. Lezama and T. Rojo, *Angew. Chem., Int. Ed. Engl.*, 1996, **35**, 78.
- 7 S. Han, J. L. Manson, J. Kim and J. S. Miller, *Inorg. Chem.*, 2000, **39**, 4182.
- 8 S. Martin, M. G. Barandika, L. Lezama, J. L. Pizarro, Z. E. Serna, J. I. R. de Larramendi, M. I. Arriortua, T. Rojo and R. Cortes, *Inorg. Chem.*, 2001, **40**, 4109.
- 9 A. Escuer, R. Vicente, F. A. Mautner, M. A. S. Goher and M. A. M. Abu-Youssef, *Chem. Commun.*, 2002, 64.
- 10 M. A. M. Abu-Youssef, M. Drillon, A. Escuer, M. A. S. Goher, F. A. Mautner and R. Vicente, *Inorg. Chem.*, 2000, **39**, 5022.
- 11 Z. Shen, J. L. Zuo, Z. Yu, Y. Zhang, J. F. Bai, C. M. Che, H. K. Fun, J. J. Vittal and X. Z. You, *J. Chem. Soc., Dalton Trans.*, 1999, 3393.
- 12 R. Cortes, L. Lezama, J. L. Pizarro, M. I. Arriortua, X. Solans and T. Rojo, *Angew. Chem., Int. Ed. Engl.*, 1994, **33**, 2488.
- 13 M. Abu Youssef, A. Escuer, M. A. S. Goher, F. A. Mautner and R. Vicente, *J. Chem. Soc., Dalton Trans.*, 2000, 413.
- 14 M. A. M. Abu-Youssef, A. Escuer, M. A. S. Goher, F. A. Mautner, G. J. Reiss and R. Vicente, *Angew. Chem., Int. Ed.*, 2000, **39**, 1624.
- 15 E. Q. Gao, S. Q. Bai, Z. M. Wang and C. H. Yan, *J. Am. Chem. Soc.*, 2003, **125**, 4984.
- 16 R. Cortes, J. L. Pizarro, L. Lezama, M. I. Arriortua and T. Rojo, *Inorg. Chem.*, 1994, **33**, 2697.
- 17 T. K. Karmakar, B. K. Ghosh, A. Usman, H.-K. Fun, E. Rivière, T. Mallah, G. Aromí and S. K. Chandra, *Inorg. Chem.*, 2005, **44**, 2391.
- 18 Z. H. Zhang, X. H. Bu, Z. H. Ma, W. M. Bu, Y. Tang and Q. H. Zhao, *Polyhedron*, 2000, **19**, 1559.
- 19 Z. H. Ni, H. Z. Kou, L. Zheng, Y. H. Zhao, L. F. Zhang and R. J. Wang, *Inorg. Chem.*, 2005, **44**, 4728.
- 20 A. C. T. North, D. C. Phillips and F. S. Mathews, *Acta Crystallogr., Sect. A*, 1968, **24**, 351.
- 21 *SAINTE*, v6.02, Bruker AXS, Madison, WI, USA, 1999.
- 22 *International Tables for Crystallography*, Kluwer Academic Publishers, Dordrecht, The Netherlands, 1992.
- 23 G. M. Sheldrick, in *SHELX-97, Program for Solution of Crystal Structure*, University of Göttingen, Germany, 1997.
- 24 L. J. Farrugia, *J. Appl. Crystallogr.*, 1997, **30**, 565.
- 25 M. A. M. Abu-Youssef, A. Escuer, M. A. S. Goher, F. A. Mautner and R. Vicente, *Eur. J. Inorg. Chem.*, 1999, 687.
- 26 A. Escuer, R. Vicente, M. A. S. Goher and F. A. Mautner, *Inorg. Chem.*, 1998, **37**, 782.
- 27 A. Escuer, R. Vicente, M. A. S. Goher and F. A. Mautner, *Inorg. Chem.*, 1997, **36**, 3440.
- 28 E. Q. Gao, Y. F. Yue, S. Q. Bai, Z. He and C. H. Yan, *J. Am. Chem. Soc.*, 2004, **126**, 1419.
- 29 O. Kahn, *Molecular Magnetism*, VCH, New York, 1993.
- 30 E. Q. Gao, S. Q. Bai, Y. F. Yue, Z. M. Wang and C. H. Yan, *Inorg. Chem.*, 2003, **42**, 3642.